https://doi.org/10.20965/jrm.2023.p0734

Paper:

Through-Hole Detection and Finger Insertion Planning as Preceding Motion for Hooking and Caging a Ring-Shaped Objects

Koshi Makihara*, Takuya Otsubo, and Satoshi Makita*****

*Osaka University
1-3 Machikaneyama, Toyonaka, Osaka 560-8531, Japan
E-mail: makihara@hlab.sys.es.osaka-u.ac.jp
**National Institute of Technology, Sasebo College
1-1 Okishincho, Sasebo, Nagasaki 857-1193, Japan
***Fukuoka Institute of Technology
3-30-1 Wajiro-higashi, Higashi-ku, Fukuoka, Fukuoka 811-0295, Japan
E-mail: makita@fit.ac.jp
[Received December 1, 2022; accepted March 29, 2023]

This study investigated a pregrasp strategy for hooking and caging ring-shaped objects. Through-hole features enable the robot hand to hook an object with holes by inserting its finger into one of the holes. Compared to directly grasping the ring, an inserting motion is more convenient to allow the uncertainty of positioning errors and avoid collisions between the hand and the object. Instead of recognizing the exact shape of the object, we only detected its ring-shaped feature as a through-hole to be inserted and estimated its approximate center position and orientation from the point cloud of the object. The estimated geometric properties enabled the approaching motion of the robotic gripper to complete insertion. The proposed perception and motion-planning method was demonstrated for rigid and deformable objects with holes.

Keywords: caging, manipulation, objects with holes, perception, motion planning

1. Introduction

In recent years, robotic manipulators have been expected to work for production in industrial factories and for human-like services [1, 2]. Robots should grasp and manipulate numerous kinds of everyday objects with different shapes, materials, masses, and sizes. Because robots often have hardware limitations, such as their reaching range and hands with low degrees of freedom, completing the assigned tasks can be challenging in certain instances.

Many studies have addressed these difficulties from the viewpoint of object perception and grasp planning. Unknown objects to be grasped can often be detected and identified from depth images for motion planning [3], and a motion planner using a deep-learning method can generate appropriate grasp poses [4]. These approaches perform with robotic systems in real-world applications, such as industrial production [5] and warehouse automation [6]. More stable grasp performances require absorbing the sensor noises in object perception and motion planning, and errors in robot control should also be avoided.

This study focuses on robotic caging, which is a grasping method that considers geometric constraints [7]. In this method, the robot bodies surround a target object to prevent it from escaping the cage formed by the robots. This capturing strategy can be achieved even by position-controlled robots because such geometric constraints do not offer any force equilibrium and force control except for avoiding excessive internal forces. Caging grasps are often used for preshaping poses of grasping [8, 9]. This can then provide margins for uncertainty caused by perception and control errors [10]. Owing to the above advantages of geometric constraints, caging grasps by robotic hands in three-dimensional space have been proposed. Makita et al. derived sufficient conditions for the caging of certain classified primitive shapes and planned a sequential caging-based manipulation [11, 12]. Other caging grasps also focus on the shape features of objects, such as a topological approach for necked shapes [13] and ring shapes [14]. Kwok et al. proposed a rope-wrapping constraint for both the ring and neck shapes [15]. In contrast to *complete* caging grasps in two-dimensional space, caging by robot hands in the three-dimensional space does not often satisfy the necessary conditions owing to hardware limitations, such as the few fingers in parallel jaw grippers and hands with low degrees of freedom. Hence, *partial* caging has been studied to allow the incompleteness of geometric constraints [16, 17]. Partially caged objects have paths that allow escape from the cage; however, the gravitational and contact forces interfere with the objects not escaping [18, 19]. The hooking strategy, in which a robot captures ring-shaped objects with only

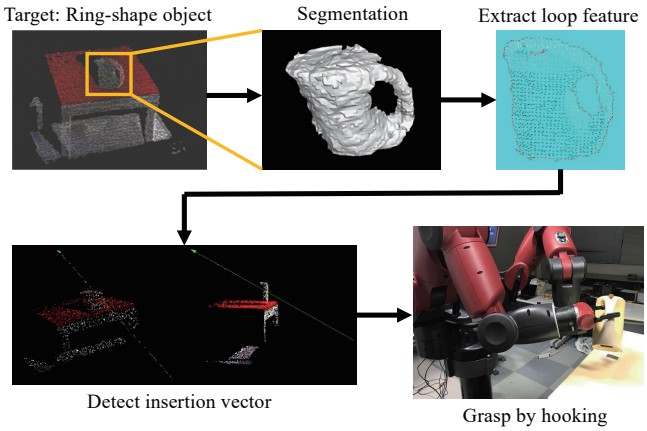

Fig. 1. Planning of *ring-type caging* via finger insertion motion: using point cloud data from a depth camera, the target object on the table is segmented and detected with its through-hole features. Finally, the insertion motion is demonstrated using a robotic arm and a parallel jaw gripper.

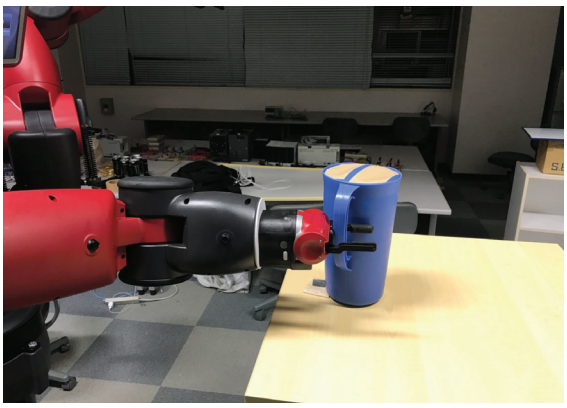

Fig. 2. Example of preceding motion for *ring-type caging* and hooking. The insertion motion requires the position and orientation of the through-hole of the object.

a few fingers and resists gravitational forces, is an intuitive approach for grasping and catching objects [20, 21]. These require detecting ring-shaped features to obtain the contact points of grasping or the insertion points of fingers, as in the case of ring-type caging presented in [12].

In this study, we investigate the insertion planning of a robotic jaw gripper into object holes for hooking motions as preshaping of caging grasps (**Fig. 1**). The shape features of the hole, used as geometric information required to insert one of the fingers, were estimated with depth images using point cloud processing. We verified the proposed method for shape-feature detection and motion planning using everyday objects. In fact, there are certain unsuitable situations for applying caging grasps, such as holding a water-filled mug, because the posture of the grasped object is often not fixed in caging grasps. Nevertheless, this intuitive grasping strategy has advantages attributed to geometric constraints in particular scenes.

The main contribution of this study is an attempt to detect holes and determine the insertion target point and direction without any approximation by the primitive shapes of objects. In general, the shapes of holes in three-dimensional space are not always straightforward, particularly for the estimated shapes from the noised point cloud. Hence, determining an appropriate insertion target point to avoid collisions with the object is difficult. In addition, some holes cannot be pass through. For example, a mug has two holes in its handle and lip; however, the lip hole is inappropriate for finger insertion. Although it is possible to hook the object at the lip, the handle is more suitable for hooking motions and preshaping of caging. These can be distinguished by projecting the point cloud onto the plane. Moreover, we estimated the insertion abstract point using the circumscribed cuboid of the through-hole and determined the insertion direction for the hole using each normal direction on its contour. Motion planning using the above geometric information is not novel and employs a conventional motion planner with random sampling.

2. Sufficient Conditions of Caging Grasp for Objects with Holes

According to a survey paper on robotic caging [7], there are various types of caging grasps by a multifingered hand, focusing on target object features and capturing strategies. Furthermore, sufficient conditions of caging grasps have been studied for each categorized pattern of object constraint. This study deals with *caging an object with holes* [14], which is also called *ring-type caging* [12], in which a robotic finger is inserted into one of the holes and approaches the other bodies of the robots. When the gap between the approaching robot bodies becomes sufficiently narrow for the object to not pass through the gap, the object is geometrically confined. These sufficient conditions guarantee the construction of Hopf link [a] with the hole of the object and the robotic fingers, similar to a chain. If the robots are fully position-controlled with an infinite servo torque, the object will never escape from the robotic cage without considering the force equilibrium.

Inserting the robotic finger into the through-hole is the preceding motion before completing the caging of a ring-shaped object. However, only the insertion motion can accomplish hooking capturing as partial caging, even by a robotic jaw gripper whose fingers have no joints to form a ring shape (**Fig. 2**). In this study, we focus on the preceding motion and the geometric features necessary to plan finger insertion.

3. Methodology

This study assumes that a target object has a through-hole for finger insertion. For the insertion strategy, we determine the insertion position and direction toward the hole of the object. The geometric information required

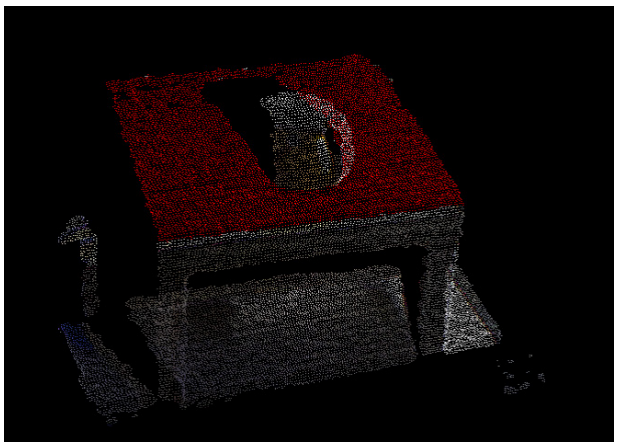

Fig. 3. Example of the plane segmentation: the largest plane is detected on which the target object assumes to be present.

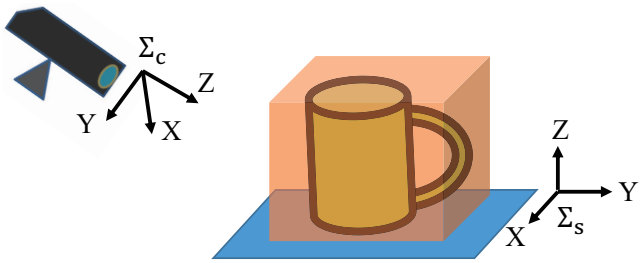

Fig. 4. Removal process of unnecessary point cloud. The coordinate system of the sensor is $\sum_c$, whereas that of the plane is $\sum_s$. The estimated bounding box of the target object is represented by the cuboid.

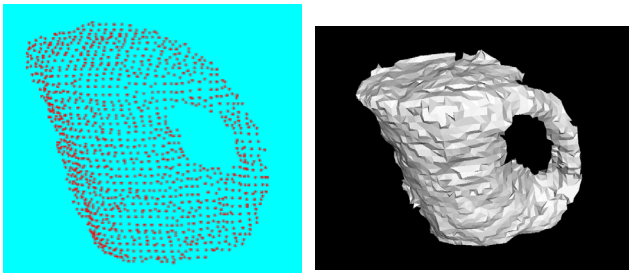

(a) Segmentation of the target object (b) Meshed point cloud

Fig. 5. Object detection and surface estimation for the target object.

for motion planning is estimated using the point cloud of the object obtained by an RGB-D camera. Note that the detailed shape of the target object nor the recognition of the object itself is not required because these are not necessary for inserting the robotic finger into the hole. However, the approximate shape of the object represented by the point cloud is essential to avoid collisions between the robot and the object during insertion. Additionally, we assume that the robotic finger and manipulator used in this study are fully position-controlled with sufficiently high servo torques to resist any external wrench applied during manipulation.

3.1. Perception of Ring-Shaped Objects

3.1.1. Object Detection from Point Cloud

Three-dimensional (3D) object detection is a key issue in planning robotic grasping and manipulation [22–25], and there are various efficient approaches using point clouds retrieved by RGB-D cameras. In this study, object detection methods are irrelevant, and we assume that the segmentation of point clouds can be accomplished using certain approaches to retrieve the sufficient 2.5D image of the target object. Although the heuristic procedure for extracting the focused point cloud in this study is trivial, employing this approach is not always necessary.

For simplicity, we assume that the target object with holes is on a flat table, and a depth camera detects the table as the largest plane in the three-dimensional scene. After acquiring the point cloud of the scene using the depth camera, plane equation fitting is performed to detect flat surfaces in the scene. Among the areas of all the planes, the largest plane segmentation is selected as the assumed table on which the target object is placed (**Fig. 3**). The plane extraction algorithm then reserves only the point cloud existing over the largest plane in the plane coordinate (**Fig. 4**). Thus, the remains correspond to all the objects on the flat table and often include multiple objects. Hence, a labeling algorithm is run to separate the point cloud into clusters to identify each object.

When multiple objects are present on the flat plane, the target object must be recognized from the clusters. Although the following algorithm for detecting through-hole features is applicable to any cluster of point clouds, the target was deliberately selected for simplicity. The dominant choice is not required when only one target object has holes.

The extracted cluster of the point cloud represents its discrete location on the surface of target object (**Fig. 5(a)**). Thus, a meshing algorithm is run to construct a polygon mesh as the estimated surface of the target (**Fig. 5(b)**).

3.1.2. Recognition of Through-Hole Features

This section aims to identify the through-holes of the object as ring-shaped features in the polygon mesh, which is composed of triangles and represents a 2.5-dimensional approximated surface of the target object. Because we obtain a point cloud from only one shot of the depth camera, we do not obtain the entire target surface. The edges of the triangles are grouped into two types of line segments: a shared line between the two triangles and a boundary line facing the outside (see the left side of **Fig. 6**). The boundary line segments generally represent the contours of the polygon mesh, and the outer line segments must be looped. In addition, the polygon mesh has an inner looped boundary contour, as shown on the right side of **Fig. 6**. Thus, the proposed method for recognizing the through-holes of the object involves detecting the nesting loop contours on the polygon mesh of the object.

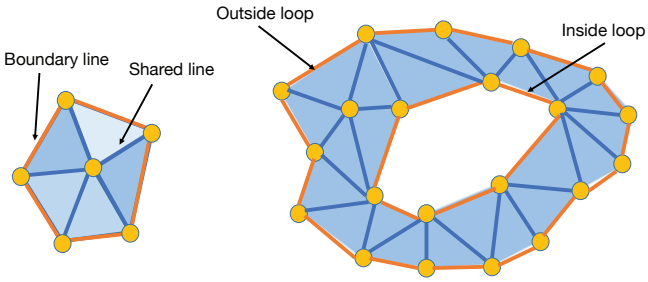

Fig. 6. Description of extracting the loop features.

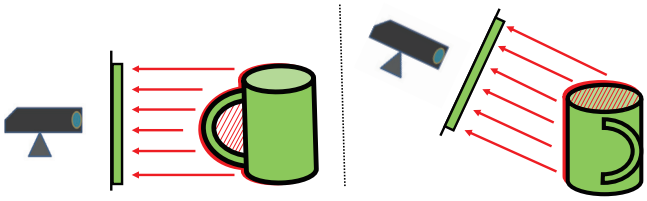

Fig. 7. Examples of unnecessary loops by projection onto 2D plane.

However, noised point clouds induce incompletely looped contours in three-dimensional space. In addition, some looped contours do not correspond to through-holes, such as mug lips. Hence, before polygon mesh processing, the point cloud is projected onto the vertical plane of the optical axis of the depth camera to avoid such errors. This process can remove unnecessary looped boundary lines and discover through-holes visible to the camera (**Fig. 7**). After projection, we obtain the *point cloud on the two-dimensional plane* and generate a planar mesh. Hence, we can quickly draw *complete* looped contours from the mesh.

Moreover, we employ the following smoothing technique. We assume that the estimated looped contour contains separate line segments whose either endpoint is present within a certain distance from the estimated looped contour. Tiny looped contours with less than ten edges are neglected. In obtaining two-looped nesting contours, a through-hole in the object can be found from the camera view of the three-dimensional scene. Otherwise, the object is assumed to have no through-holes, whether they are visible in the camera view.

In **Fig. 8**, we show an example in which a kettle is scanned, and the looped contours representing its handle can be successfully detected. Note that there are multiple inner-looped contours in the mesh polygon at times, which implies that the target object may have multiple through-holes as candidates for finger insertion. In this study, we do not narrow down the candidates for motion planning and deliberately select one. A more effective selection that considers collision detection and task recovery strategies is expected in the future.

It should be noted that the through-hole detection does not consider the possibility of finger insertion, as discussed in the next section. To pass through the hole, the robotic finger must not occupy the body of the object.

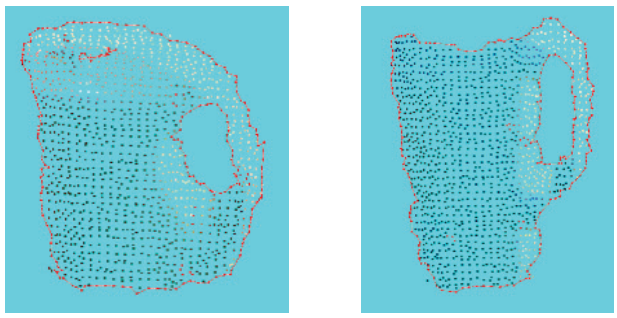

Fig. 8. Results of extracting through-hole features.

When the cross-section of the finger is larger than that of the through-hole, a failure can be expected. However, it is difficult to determine the cross-section of complicated loops in three-dimensional space along the finger insertion direction. Additionally, because we cannot obtain the entire three-dimensional image of the object from only a one-sided depth image, the true cross-section is not confirmed. Hence, we do not derive the shape restriction between the object and robots in this step and practically adopt collision avoidance.

3.2. Planning of Finger Insertion Motion

Using the through-hole features, we consider motion planning for inserting a robotic finger into the hole as the preceding motion for hooking and ring-type caging. The insertion motion requires a reaching point of the finger and a corresponding direction vector as geometric information. Although we can obtain the through-hole features in three-dimensional space as in the previous procedure, their forms are generally complicated and not straightforward. Hence, we determine the approximate position and orientation of the hole instead of estimating its exact form. The following procedure can work in many situations because finger insertion into the hole often has sufficient tolerance to avoid collisions between the finger and the body of the hole.

3.2.1. Determination of Reaching Point

When a robotic finger approaches the through-hole of the target object, collision avoidance between them should be considered. Because it is difficult to determine an optimal reaching point for the complicated shape of the hole, we only determine an approximate central point of the hole as the furthest point from the body of the hole to avoid any collisions. Accordingly, we obtain a circumscribed cuboid of the through-hole contour and determine its center point as the reaching point for the finger (**Fig. 9**). Note that this estimation is unsuitable for gourd-shaped holes because the center point of each circumscribed cuboid may be around its neck. To avoid collision with the approaching finger and the body of the hole, the reaching point around the broader area of the hole must be determined. This may require separating the hole into convex shapes.

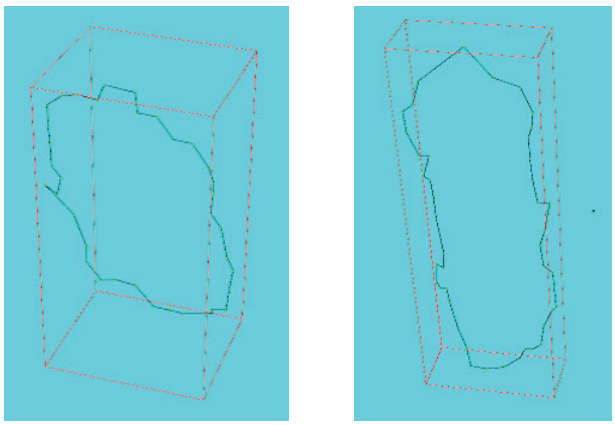

Fig. 9. Circumscribed cuboid of the through-hole corresponding to the results in **Fig. 8**.

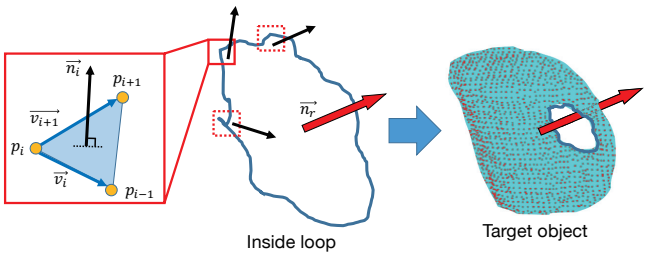

Fig. 10. Description of detecting insertion vector.

3.2.2. Determination of Insertion Direction

The insertion direction of the robotic finger must avoid collisions with the object until the finger reaches the location determined in the previous section. The optimal direction for the insertion is almost perpendicular to the hole contour. Hence, we focus on the estimated contours that consist of line segments. Two adjacent line segments are selected, and two direction vectors along the line segments from the intersection point are obtained (**Fig. 10**). It calculates the two vectors $\boldsymbol{v}_i$ from a target point $\boldsymbol{p}_i$ in the loop to an adjacent point $\boldsymbol{p}_{i-1}$ and $\boldsymbol{v}_{i+1}$ from $\boldsymbol{p}_i$ to another adjacent point $\boldsymbol{p}_{i+1}$ and estimates the outer product $\boldsymbol{n}_i = \boldsymbol{v}_i \times \boldsymbol{v}_{i+1}$. The normal vector of the two selected line segments on contour $\boldsymbol{n}_i$ can be calculated for every intersection point. Finally, we obtain the representative normal vector $\boldsymbol{n}_r = \sum_{k=1}^{N} \boldsymbol{n}_k$, which is assumed to be almost perpendicular to the hole. The sign of the calculated vector should be adjusted using the inner product of the vectors for the appropriate insertion direction. The normalized and aligned normal vectors of the hole can be expressed as follows:

$$\hat{\boldsymbol{n}}_r = sign\left((\boldsymbol{p}_l - \boldsymbol{p}_h) \cdot \boldsymbol{n}_r\right) \frac{\boldsymbol{n}_r}{||\boldsymbol{n}_r||}, \quad \ldots\ldots\ldots \quad (1)$$

where $\boldsymbol{p}_l$ denotes the estimated position of the hole, as described in the previous section, and $\boldsymbol{p}_h$ denotes the initial position of the robotic hand. The results for the detected insertion directions are shown in **Fig. 11**. Four other views of the same object are also shown in the figure. The arrows indicate the estimated direction through the hole.

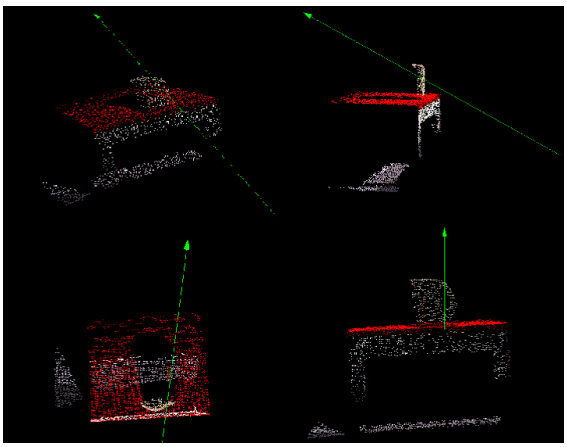

(a) Kettle

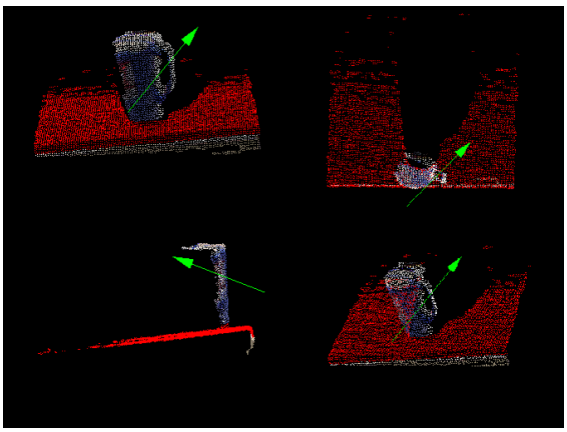

(b) YCB kettle

Fig. 11. Results of estimating insertion direction. Each figure provides the same result from four other viewpoints.

3.2.3. Insertion Strategy

The finger insertion motion of the robotic gripper is determined using the above calculated geometric specifications: the approximate position and estimated normal vector of the hole. The finger insertion motion is a preceding motion for hooking or ring-type caging. Note that we do not consider the collision between the robot and the object during insertion in this step. Based on the insertion strategy, the employed motion planner searches for the motion path of the robot while considering collision avoidance. The following steps describe the insertion strategy (**Fig. 12**):

Step 1 The robot finger approaches from the initial position $\boldsymbol{p}_h$ to a waypoint $\boldsymbol{p}_w$. The waypoint is determined to be the nearest position in front of the hole as $\boldsymbol{p}_w = \boldsymbol{p}_l - a\hat{\boldsymbol{n}}_r$, where a is an arbitrary positive value.

Step 2 The hand of the robot changes its posture to align the direction of the finger body $\boldsymbol{d}_{fng}$ parallel to the direction vector $\hat{\boldsymbol{n}}_r$.

Step 3 The finger moves from $\boldsymbol{p}_w$ to $\boldsymbol{p}_l$ along $\hat{\boldsymbol{n}}_r$ without changing its posture.

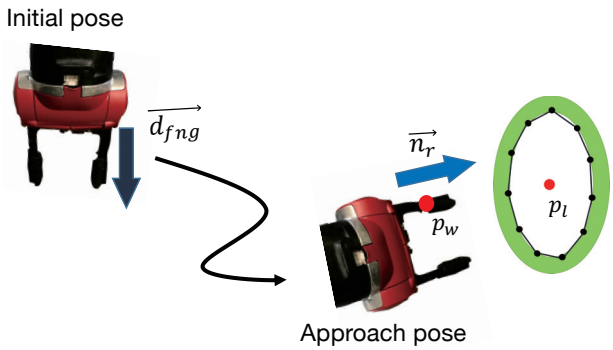

Fig. 12. Planning of finger insertion into the through-hole.

Fig. 13. Target rigid and deformable ring-shaped objects.

The represented finger point should then be located as close to the palm as possible for the entire body of the finger to pass through the hole.

After finger insertion, the robotic hand lifts the target object and moves vertically. This method is called hooking, as proposed by Stork [20], and it can constrain an object using gravitational forces. Gravity-aided grasping with incomplete geometric constraints has also been studied for *energy-bounded caging* [18], *basket caging* [19], and *partial caging* [16].

4. Experimental Results

We demonstrate the motion of four objects with holes, as shown in **Fig. 13**, to validate the proposed insertion strategy for the robotic finger as the preceding motion of hooking and ring-type caging. Each has only one though-hole for insertion. The blue kettle is one of YCB object [26], which is refereed to here as "YCB kettle," whereas the other kettle is simply called a "kettle." The tote bag and cable are deformable objects. Note that the YCB object and model set are presented for benchmarking in robotic grasping and manipulation research [26], which include everyday objects of various sizes, weights, and shapes to assess the manipulation performances.

4.1. Hardware and Software Setup

In the experiments, we use a Kinect v1 (Microsoft Corp.) as the depth camera to obtain a point cloud. A dual-arm robot with parallel-jaw grippers, Baxter (Rethink Robotics Inc.), is used as the manipulator. The entire sequence of perception, motion planning, and robot control is implemented with ROS (Robot Operating System [27]).

The control system runs on an Ubuntu 14.04 PC with a CPU of Intel Core i5 running at 2.8 GHz.

4.2. Results of Perception and Motion Planning

Figure 14 shows the results of synthesis planning from perception to motion. For each trial, the target objects are located at marginally different placements inside the workspace of the manipulator. The handles of the kettles and tote bag are located nearly vertical to the optical axis of the depth camera for the camera to acquire the point cloud on the handles. Thus, the shape of the tote bag handle changed every time owing to the gravitational force. By contrast, the rolled cable lay on the desk and is deformed at times. In addition, the robot performs a lifting motion to pick up the target object as hooking. The number of finger insertion trials for each object is ten, and the success rates are as follows: $7/10$, $8/10$, $5/10$, $0/10$ for the kettle, YCB kettle, tote bag, electric cable, respectively. Most failures occurred during finger insertion with collisions between the robot and the object, although the geometric information of the holes was successfully estimated. The main reason for the failures with the electric cable was the faulty determination of the insertion direction, as shown in **Fig. 15**. In this case, the point cloud segmentation, which was supposed to separate the cable and the desk, failed. Moreover, the largest through-hole to be inserted was not determined. Another tiny through-hole was obtained, and its representative direction was estimated.

4.3. Discussion

All experiments, except for the rolled cable, showed that the proposed method could successfully detect each through-hole of the target objects with marginally different placements and generate finger insertion motion for each object to hook up. Because each ground truth value of the reference points of the loops and the corresponding insertion direction were not determined, as mentioned in Section 3.2, this study was only verified qualitatively without comparing the estimation precision.

Contacts between the finger and the target object during the planned insertion motion caused failures. Factors

(a) Kettle (b) YCB kettle

(c) Tote bag

Fig. 14. Experimental results of motion planning for finger insertion.

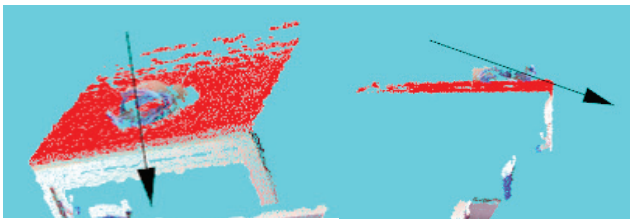

Fig. 15. This case fails to generate the trajectory. The insertion direction is not estimated for the largest through-hole of the cable but for any scattered features.

for these failures were the error from the sensor noises and the lack of point cloud density when calculating the polygon mesh. In addition, the area of the through-hole affected the success rate. The width of the through-hole of the kettle's handle was 27.3 mm, whereas that of the YCB kettle was 17.2 mm. The gripper, on the other hand, has a width of 12.3 mm. If the insertion direction is excessively tilted for the hole, motion planning may not be completed owing to the collision between the finger and the object. Nevertheless, in these experiments, the insertion planning and hooking motion could be performed successfully in certain instances, even with collisions. The margin in the finger insertion strategy for the through-hole can contribute to absorbing such uncertainties in object perception. Moreover, in the case of the tote bag, the deformation caused by the collision with the finger sometimes did not interrupt the planned finger insertion (**Fig. 14(c)**).

In the case of the cable, there were no successful trials, despite being rarely deformed. The main reason for this failure is that the cable was placed on the desk to cover its largest through-hole, as shown in **Fig. 13(d)**. **Fig. 15** shows an unexpected estimation of the through-holes and insertion direction in such cases. Even if the finger insertion into the cable placed on the desk can be performed, the hooking motion used to lift the object by the straightforward approach described in Section 3.2.3 may fail. Thus, the target object with holes should be present such that a depth camera can observe its through-holes, and point cloud segmentation succeeds in the proposed method. Furthermore, we must improve the determination of the insertion direction for various poses of through-holes and path planning, considering collision avoidance, for more stable finger insertion.

5. Conclusion

In this study, we proposed perception and planning methods to obtain finger insertion motion for ring-shaped objects with through-holes as a preceding motion of hooking and ring-type caging. A projection technique for a point cloud facilitated the detection of the through-holes. The position of the through-hole was determined to be at the center of the circumscribed cuboid of the hole. The insertion direction was estimated for each normal direction of the line segments comprising the hole contour. We demonstrated the generated motion for inserting a robotic finger into the hole using four objects.

In the future, we plan to apply this method to various objects in complex environments and improve point cloud segmentation and feature detection. Collision avoidance and deformation of the target object are also considered for more stable grasping and manipulation.

Acknowledgments

This work was supported by JSPS KAKENHI JP17H04669.

References:

[1] Y. Domae, "Recent trends in the research of industrial robots and future outlook," J. Robot. Mechatron., Vol.31, No.1, pp. 57-62, 2019. https://doi.org/10.20965/jrm.2019.p0057

[2] M. Shintani, Y. Fukui, K. Morioka, K. Ishihata, S. Iwaki, T. Ikeda, and T. Lüth, "Object grasping instructions to support robot by laser beam one drag operations," J. Robot. Mechatron., Vol.33, No.4, pp. 756-767, 2021. https://doi.org/10.20965/jrm.2021.p0756

[3] A. Saxena, J. Driemeyer, and A. Y. Ng, "Robotic grasping of novel objects using vision," The Int. J. of Robotics Research, Vol.27, No.2, pp. 157-173, 2008. https://doi.org/10.1177/0278364907087172

[4] I. Lenz, H. Lee, and A. Saxena, "Deep learning for detecting robotic grasps," The Int. J. of Robotics Research, Vol.34, No.4-5, pp. 705-724, 2015. https://doi.org/10.1177/0278364914549607

[5] Y. Domae, A. Noda, T. Nagatani, and W. Wan, "Robotic general parts feeder: Bin-picking, regrasping, and kitting," IEEE Int. Conf. on Robotics and Automation, pp. 5004-5010, 2020. https://doi.org/10.1109/ICRA40945.2020.9197056

[6] J. Mahler, M. Matl, V. Satish, M. Danielczuk, B. DeRose, S. McKinley, and K. Goldberg, "Learning ambidextrous robot grasping policies," Science Robotics, Vol.4, No.26, Article No.eaau4984, 2019. https://doi.org/10.1126/scirobotics.aau4984

[7] S. Makita and W. Wan, "A survey of robotic caging and its applications," Advanced Robotics, Vol.31, No.19-20, pp. 1071-1085, 2017. https://doi.org/10.1080/01691864.2017.1371075

[8] E. Rimon and A. Blake, "Caging planar bodies by one-parameter two-fingered gripping systems," The Int. J. of Robotics Research, Vol.18, No.3, pp. 299-318, 1999. https://doi.org/10.1177/02783649922066222

[9] R. Diankov, S. S. Srinivasa, D. Ferguson, and J. Kuffner, "Manipulation planning with caging grasps," 8th IEEE-RAS Int. Conf. on Humanoid Robots, pp. 285-292, 2008. https://doi.org/10.1109/ICHR.2008.4755966

[10] W. Wan, R. Fukui, M. Shimosaka, T. Sato, and Y. Kuniyoshi, "Grasping by caging: A promising tool to deal with uncertainty," 2012 IEEE Int. Conf. on Robotics and Automation, pp. 5142-5149, 2012. https://doi.org/10.1109/ICRA.2012.6224676

[11] S. Makita and Y. Maeda, "3D multifingered caging: Basic formulation and planning," Proc. of IEEE/RSJ Int. Conf. on Intelligent Robots and System, Nice, France, pp. 2697-2702, 2008. https://doi.org/10.1109/IROS.2008.4650895

[12] S. Makita, K. Okita, and Y. Maeda, "3D two-fingered caging for two types of objects: Sufficient conditions and planning," Int. J. of Mechatronics and Automation, Vol.3, pp. 263-277, 2013. https://doi.org/10.1504/IJMA.2013.058376

[13] A. Varava, D. Kragic, and F. T. Pokorny, "Caging grasps of rigid and partially deformable 3-d objects with double fork and neck features," IEEE Trans. on Robotics, Vol.32, No.6, pp. 1479-1497, 2016. https://doi.org/10.1109/TRO.2016.2602374

[14] F. T. Pokorny, J. A. Stork, and D. Kragic, "Grasping objects with holes: A topological approach," IEEE Int. Conf. on Robotics and Automation, pp. 1100-1107, 2013. https://doi.org/10.1109/ICRA.2013.6630710

[15] T.-H. Kwok, W. Wan, J. Pan, C. C. L. Wang, J. Yuan, K. Harada, and Y. Chen, "Rope Caging and Grasping," Proc. of IEEE Int. Conf. on Robotics and Automation, Stockholm, Sweden, pp. 1980-1986, 2016. https://doi.org/10.1109/ICRA.2016.7487345

[16] T. Makapunyo, T. Phoka, P. Pipattanasomporn, N. Niparnan, and A. Sudsang, "Measurement framework of partial cage quality based on probabilistic motion planning," Proc. of IEEE Int. Conf. on Robotics and Automation, Karlsruhe, Germany, pp. 1574-1579, 2013. https://doi.org/10.1109/ICRA.2013.6630780

[17] M. Welle, A. Varava, J. Mahler, K. Goldberg, D. Kragic, and F. Pokorny, "Partial caging: a clearance-based definition, datasets, and deep learning," Autonomous Robots, Vol.45, pp. 647-664, 2021. https://doi.org/10.1007/s10514-021-09969-6

[18] J. Mahler, F. T. Pokorny, Z. Mccarthy, A. F. V. D. Stappen, and K. Goldberg, "Energy-bounded caging : Formal definition and 2-d energy lower bound algorithm based on weighted alpha shapes," IEEE Robotics and Automation Letters, Vol.1, No.1, pp. 508-515, 2016. https://doi.org/10.1109/LRA.2016.2519145

[19] A. Shirizly, E. D. Rimon, and W. Wan, "Contact space computation of two-finger gravity based caging grasps security measure," IEEE Robotics and Automation Letters, Vol.6, No.2, pp. 572-579, 2020. https://doi.org/10.1109/LRA.2020.3047773

[20] J. A. Stork, F. T. Pokorny, and D. Kragic, "A Topology-based Object Representation for Clasping, Latching and Hooking," Proc. of IEEE/RAS Int. Conf. on Humanoid Robots, pp. 138-145, 2013. https://doi.org/10.1109/HUMANOIDS.2013.7029968

[21] M. Yashima and T. Yamawaki, "Robotic nonprehensile catching: Initial experiments," Proc. of IEEE/RSJ Int. Conf. on Intelligent Robots and Systems, pp. 5480-5486, 2014. https://doi.org/10.1109/IROS.2014.6942897

[22] S. Akizuki and M. Hashimoto, "Stable position and pose estimation of industrial parts using evaluation of observability of 3D vector pairs," J. Robot. Mechatron., Vol.27, No.2, pp. 174-181, 2015. https://doi.org/10.20965/jrm.2015.p0174

[23] U. Asif, M. Bennamoun, and F. A. Sohel, "RGB-D object recognition and grasp detection using hierarchical cascaded forests," IEEE Trans. on Robotics, Vol.33, No.3, pp. 547-564, 2017. https://doi.org/10.1109/TRO.2016.2638453

[24] Y. Sakata and T. Suzuki, "Coverage motion planning based on 3D model's curved shape for home cleaning robot," J. Robot. Mechatron., Vol.35, No.1, pp. 30-42, 2023. https://doi.org/10.20965/jrm.2023.p0030

[25] R. Iinuma, Y. Hori, H. Onoyama, Y. Kubo, and T. Fukao, "Robotic forklift for stacking multiple pallets with RGB-D cameras," J. Robot. Mechatron., Vol.33, No.6, pp. 1265-1273, 2021. https://doi.org/10.20965/jrm.2021.p1265

[26] B. Calli, A. Walsman, A. Singh, S. Srinivasa, P. Abbeel, and A. M. Dollar, "Benchmarking in manipulation research: The YCB object and model set and benchmarking protocols," IEEE Robotics and Automation Magazine, Vol.22, pp. 36-52, 2015. https://doi.org/10.1109/MRA.2015.2448951

[27] M. Quigley, K. Conley, B. P. Gerkey, J. Faust, T. Foote, J. Leibs, R. Wheeler, and A. Y. Ng, "ROS: an open-source robot operating system," ICRA Workshop on Open Source Software, 2009.

Supporting Online Materials:

[a] E. W. Weisstein, "Hopf link," MathWorld – A Wolfram Web Resource. https://mathworld.wolfram.com/HopfLink.html [Accessed March 29, 2023]

Name:
Koshi Makihara

Affiliation:
Osaka University

Address:
1-3 Machikaneyama, Toyonaka, Osaka 560-8531, Japan

Brief Biographical History:

2019 Received B.E. from Advanced Course of Integrated Engineering, National Institute of Technology, Sasebo College

2021 Received M.E. in Intelligent Interaction Technologies from University of Tsukuba

Main Works:

• "Stability evaluation of subassembly considering with gravitational and frictional action," Proc. of IEEE Int. Conf. on Intelligence and Safety for Robotics (ISR), pp. 66-69, 2021.

• "Grasp pose detection for deformable daily items by pix2stiffness estimation," Advanced Robotics, Vol.36, No.12, pp. 600-610, 2022.

Membership in Academic Societies:

• Institute of Electrical and Electronics Engineers (IEEE)

• The Robotics Society of Japan (RSJ)

Name:
Takuya Otsubo

Affiliation:
National Institute of Technology, Sasebo College

Address:
1-1 Okishincho, Sasebo, Nagasaki 857-1193, Japan

Brief Biographical History:
2016 Received B.E. from National Institute of Technology, Sasebo College

Name:
Satoshi Makita

ORCID:
0000-0003-4658-8471

Affiliation:
Associate Professor, Fukuoka Institute of Technology

Address:
3-30-1 Wajiro-higashi, Higashi-ku, Fukuoka, Fukuoka 811-0295, Japan

Brief Biographical History:
2010 Received Ph.D. from Yokohama National University
2010-2020 National Institute of Technology, Sasebo College
2020- Fukuoka Institute of Technology

Main Works:
• "Offline Direct Teaching for a Robotic Manipulator in the Computational Space," Int. J. Automation Technol., Vol.15, No.2, pp. 197-205, 2021.
• "A Survey of Robotic Caging and its Applications," Advanced Robotics, Vol.31, No.19-20, pp. 1071-1085, 2017.

Membership in Academic Societies:
• Institute of Electrical and Electronics Engineers (IEEE)
• The Robotics Society of Japan (RSJ)
• The Japan Society of Mechanical Engineers (JSME)
• The Society of Instrument and Control Engineers (SICE)